Science Signaling
AAAS

Supplementary Materials for

CXCR4 signaling determines the fate of hematopoietic multipotent progenitors by stimulating mTOR activity and mitochondrial metabolism

Vincent Rondeau *et al.*

Corresponding author: Karl Balabanian, karl.balabanian@inserm.fr

Sci. Signal. **17**, eadl5100 (2024)
DOI: 10.1126/scisignal.adl5100

The PDF file includes:

Other Supplementary Material for this manuscript includes the following:

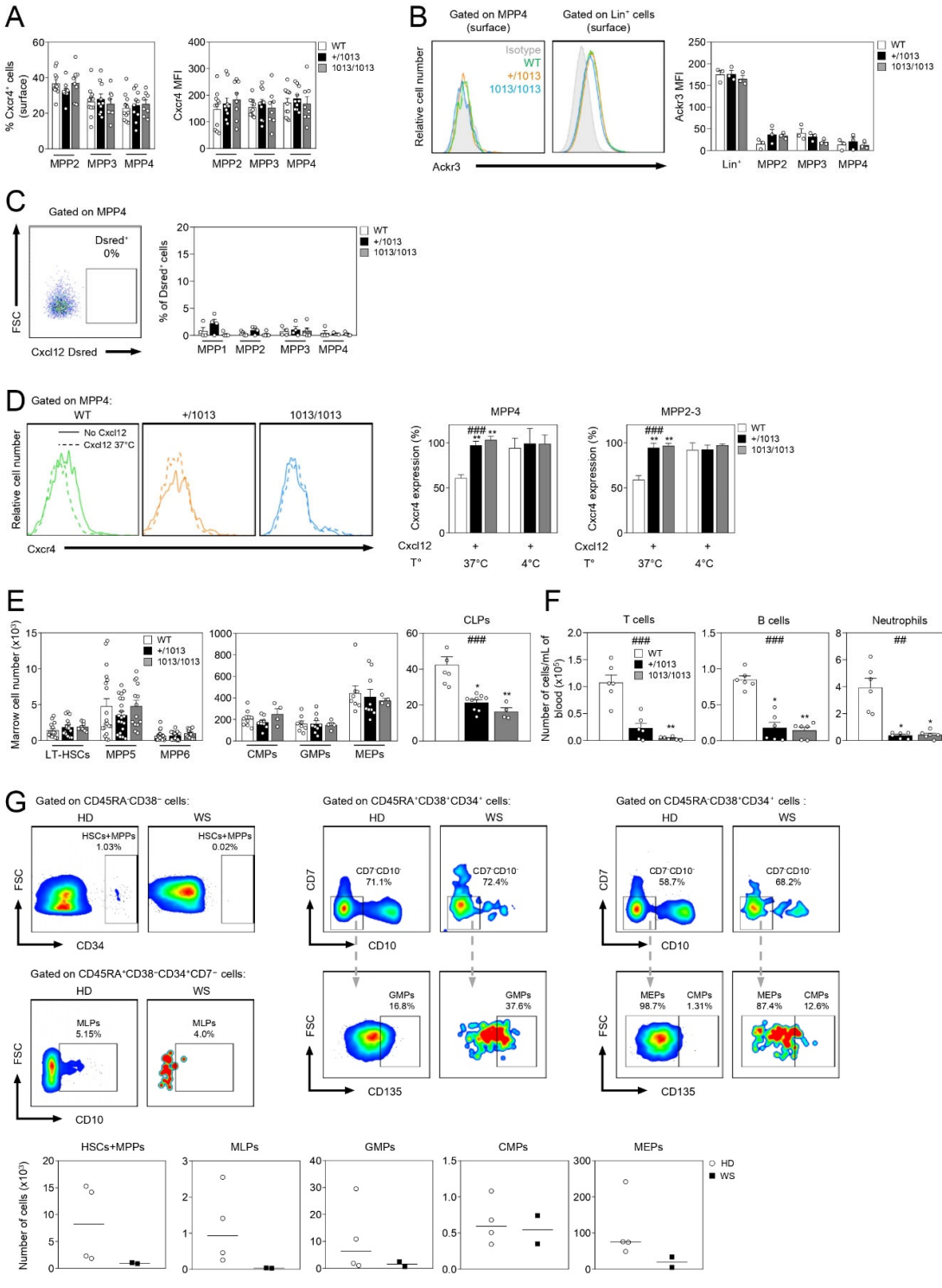
A
% Cxcr4+ cells (surface)
Cxcr4 MFI
WT
+/1013
1013/1013
MPP2 MPP3 MPP4
B
Gated on MPP4 (surface)
Gated on Lin- cells (surface)
Isotype
WT
+/1013
1013/1013
Relative cell number
Ackr3
Ackr3 MFI
Lin- MPP2 MPP3 MPP4
C
Gated on MPP4
Dsred+ 0%
FSC
Cxcl12 Dsred
% of Dsred+ cells
MPP1 MPP2 MPP3 MPP4
D
Gated on MPP4:
WT
+/1013
1013/1013
No Cxcl12
Cxcl12 37°C
Relative cell number
Cxcr4
MPP4
MPP2-3
Cxcr4 expression (%)
Cxcl12
T°
37°C
4°C
E
Marrow cell number (x10³)
LT-HSCs MPP5 MPP6 CMPs GMPs MEPs CLPs
F
T cells
B cells
Neutrophils
Number of cells/mL of blood (x10³)
G
Gated on CD45RA-CD38- cells:
HD
WS
HSCs+MPPs 1.03%
HSCs+MPPs 0.02%
FSC
CD34
Gated on CD45RA+CD38-CD34+CD7- cells:
MLPs 5.15%
MLPs 4.0%
CD10
Gated on CD45RA+CD38+CD34+ cells:
CD7 CD10- 71.1%
CD7 CD10- 72.4%
CD7
GMPs 16.8%
GMPs 37.6%
CD135
Gated on CD45RA-CD38+CD34+ cells :
CD7 CD10- 58.7%
CD7 CD10- 68.2%
MEPs 98.7%
CMPs 1.31%
MEPs 87.4%
CMPs 12.6%
HSCs+MPPs
MLPs
GMPs
CMPs
MEPs
Number of cells (x10³)
HD
WS

Fig. S1. Desensitization-resistant Cxcr4^{1013} is present on all MPP subsets. (A) Surface abundance of Cxcr4 determined by flow cytometry on MPP2, MPP3, and MPP4 from the marrow fraction of WT and Cxcr4^{1013} knockin mice. Cxcr4^{+} fractions or MFI values obtained within MPP2, MPP3, and MPP4 relative to background fluorescence based on the corresponding isotype control staining are shown. n= 4 independent experiments for a total of 11 WT, 10 +/1013, and 8 1013/1013 mice. **(B)** Representative histograms for surface detection of Ackr3 on MPP4 and Lin^{+} cells from marrow fraction of WT and knockin mice. Background fluorescence is shown (isotype, gray histogram). MFI values for Ackr3 were determined by flow cytometry on Lin^{+} cells, MPP2, MPP3, and MPP4. n= 3 independent experiments for a total of 3 mice per group. **(C)** Representative flow cytometric analysis for Dsred detection in MPP4 from marrow fraction of *Cxcl12^{Dsred}* reporter mice. Proportions of Dsred^{+} cells within MPP1, MPP2, MPP3, and MPP4 from the marrow fraction of *Cxcr4$^{+/+}$Cxcl12^{Dsred}*, *Cxcr4$^{+/1013}$Cxcl12^{Dsred}*, or *Cxcr4$^{1013/1013}$Cxcl12^{Dsred}* mice. n= 3 independent determinations for a total of 4 *Cxcr4$^{+/+}$Cxcl12^{Dsred}*, 4 *Cxcr4$^{+/1013}$Cxcl12^{Dsred}*, and 5 *Cxcr4$^{1013/1013}$Cxcl12^{Dsred}* mice. **(D)** Representative histograms for surface detection of Cxcr4 on MPP4 stimulated with Cxcl12 at 37°C for 45 min (dashed line) or incubated in medium alone (plain line). Cell surface expression of Cxcr4 on WT and Cxcr4^{1013} knockin MPP2/3 or MPP4 upon stimulation with Cxcl12 at 37°C or 4°C for 45 min. Cxcr4 expression on MPP2/3 or MPP4 incubated in medium alone was set at 100%. Data are from three independent experiments for a total of 10 WT, 10 +/1013, and 5 1013/1013 mice. **(E)** Absolute numbers of LT-HSCs, MPP5, MPP6, CMPs, GMPs, MEPs, and CLPs in the marrow fraction of WT and knockin mice. n= 5 independent experiments for a total of 15 WT, 15 +/1013, and 9 1013/1013 mice (LT-HSCs) or n= 7 independent experiments for a total of 19 WT, 19 +/1013, and 13 1013/1013 mice (MPP5/MPP6) or n= 3 independent experiments for a total of 8 WT, 9 +/1013, and 4 1013/1013 mice (CMPs/GMPs/MEPs/CLPs). **(F)** Absolute numbers of T cells (CD3^{+}), B cells (B220^{+}) and neutrophils (Gr1^{+}) in the blood of WT or knockin mice. n= 3 independent experiments for a total of 6 mice per group. **(G)** Representative dot-plots comparing the frequencies of human HSCs/MPPs, MLPs, GMPs, CMPs and MEPs. Absolute numbers of HSCs/MPPs, MLPs, GMPs, CMPs and MEPs in BM aspirates of HD and WS patients. Barplots indicate mean/SEM, horizontal lines correspond to median values. $^{\#\#}$ $P < 0.005$; $^{\#\#\#}$ $P < 0.0005$ for Kruskal–Wallis tests; * $P < 0.05$; ** $P < 0.005$ Dunn's test.

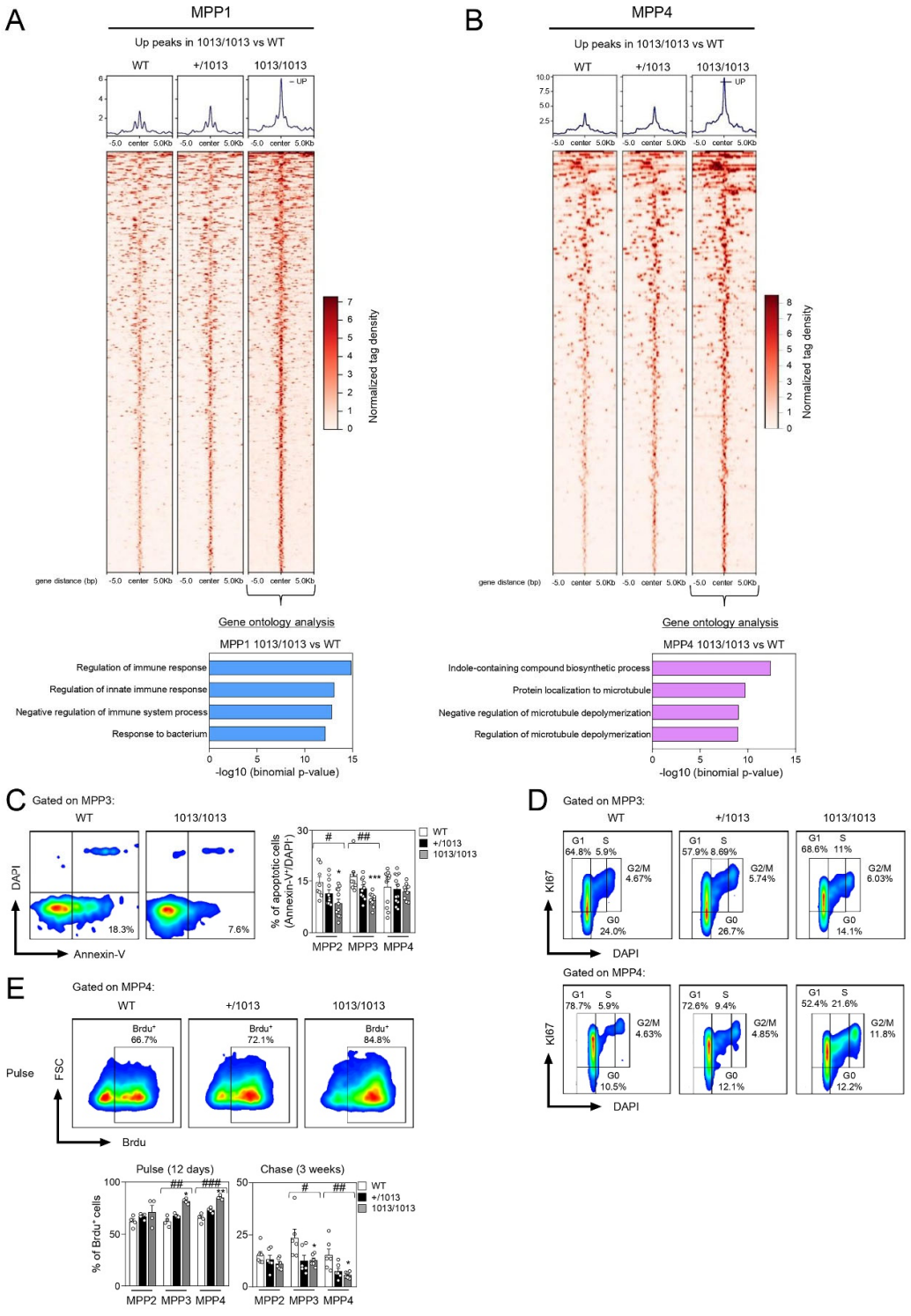
A
MPP1
Up peaks in 1013/1013 vs WT
WT
+/1013
1013/1013
UP
-5.0 center 5.0Kb
gene distance (bp)
Normalized tag density
Gene ontology analysis
MPP1 1013/1013 vs WT
Regulation of immune response
Regulation of innate immune response
Negative regulation of immune system process
Response to bacterium
-log10 (binomial p-value)
B
MPP4
Up peaks in 1013/1013 vs WT
Gene ontology analysis
MPP4 1013/1013 vs WT
Indole-containing compound biosynthetic process
Protein localization to microtubule
Negative regulation of microtubule depolymerization
Regulation of microtubule depolymerization
C
Gated on MPP3:
DAPI
Annexin-V
18.3%
7.6%
% of apoptotic cells (Annexin-V+/DAPI-)
MPP2 MPP3 MPP4
D
Gated on MPP3:
KI67
DAPI
G1 64.8% S 5.9% G2/M 4.67% G0 24.0%
G1 57.9% S 8.69% G2/M 5.74% G0 26.7%
G1 68.6% S 11% G2/M 6.03% G0 14.1%
Gated on MPP4:
G1 78.7% S 5.9% G2/M 4.63% G0 10.5%
G1 72.6% S 9.4% G2/M 4.85% G0 12.1%
G1 52.4% S 21.6% G2/M 11.8% G0 12.2%
E
Gated on MPP4:
Pulse
FSC
Brdu
Brdu+ 66.7%
Brdu+ 72.1%
Brdu+ 84.8%
Pulse (12 days)
Chase (3 weeks)
% of Brdu+ cells
MPP2 MPP3 MPP4

Fig. S2. Quiescence/cycling balance and survival profile are differentially disturbed in Cxcr4^{1013} knockin MPP subpopulations. (A) Heatmap of increased ATAC-seq peaks in WT or Cxcr4^{1013} knockin MPP1 and gene ontology analysis with associated genes. **(B)** Heatmap of increased ATAC-seq peaks in WT or knockin MPP4 and gene ontology analysis with associated genes. **(C)** Representative flow cytometric analyses comparing the frequencies of apoptotic MPP3 in WT and 1013/1013 mice. The proportions of apoptotic MPP2, MPP3, and MPP4 were determined in the marrow fraction of WT and knockin mice. n= 4 independent experiments for a total of 8 WT, 12 +/1013, and 12 1013/1013 mice. **(D)** Representative flow cytometric analyses comparing the frequencies of MPP3 and MPP4 in the different phases of the cell cycle in WT and knockin mice are shown. Data are representative of n= 5 independent experiments for a total of 15 WT, 15 +/1013, and 12 1013/1013 mice. **(E)** Representative flow cytometric analyses comparing the frequencies of BrdU^{+} MPP4 in WT and knockin mice after a 12-day pulse period. Percentage of BrdU^{+} cells among WT and knockin MPP2, MPP3, and MPP4 after a 12-days pulse period or 3 weeks of chase. n= 3 independent experiments for a total of 4 mice per group (pulse) or n= 3 independent experiments for a total of 6 mice per group (chase). $^{\#}$ $P < 0.05$; $^{\#\#}$ $P < 0.005$; $^{\#\#\#}$ $P < 0.0005$ for Kruskal–Wallis tests; * $P < 0.05$; ** $P < 0.005$; *** $P < 0.0005$ for Dunn's test compared with WT.

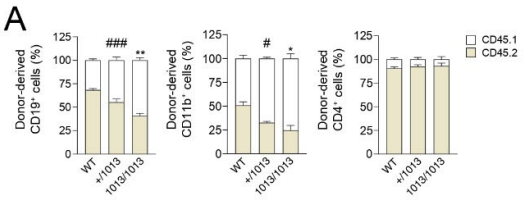
A
Donor-derived CD19+ cells (%)
Donor-derived CD11b+ cells (%)
Donor-derived CD4+ cells (%)
###
**
#
*
CD45.1
CD45.2
WT
+/1013
1013/1013

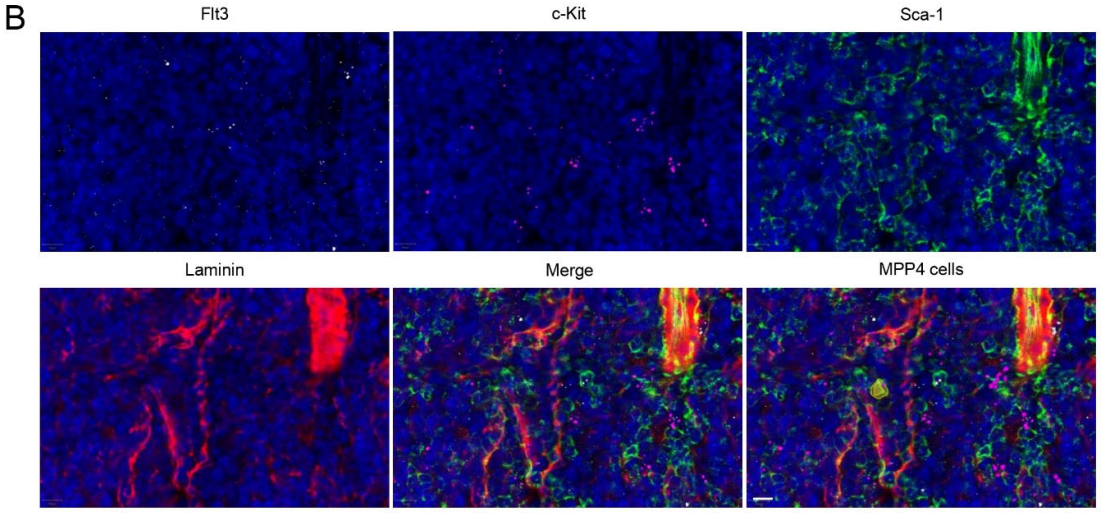
B
Flt3
c-Kit
Sca-1
Laminin
Merge
MPP4 cells

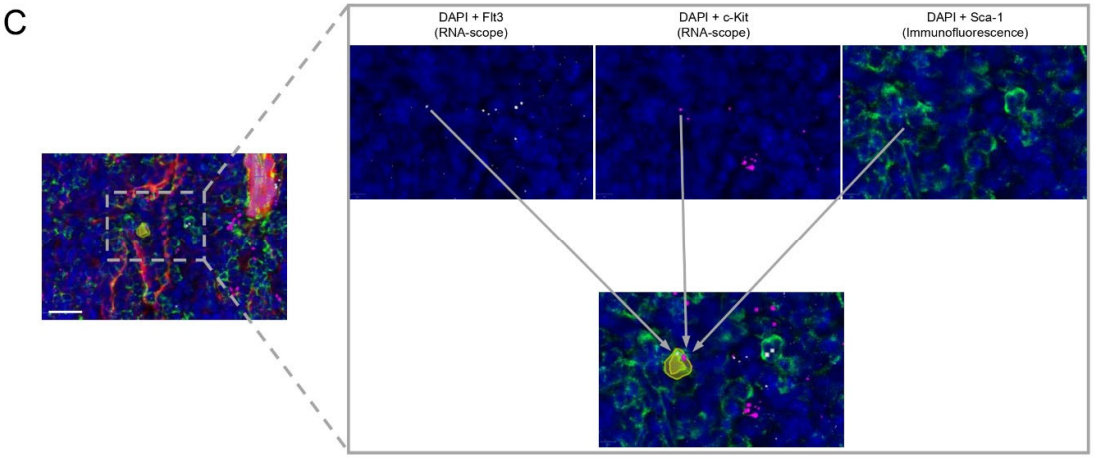
C
DAPI + Flt3
(RNA-scope)
DAPI + c-Kit
(RNA-scope)
DAPI + Sca-1
(Immunofluorescence)

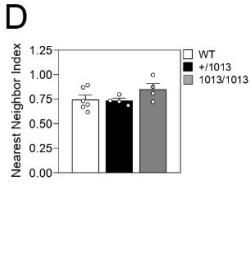
D
Nearest Neighbor Index
WT
+/1013
1013/1013

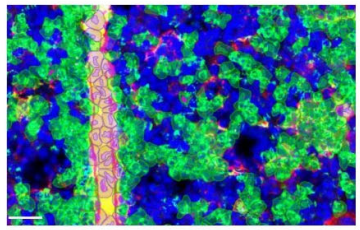
E

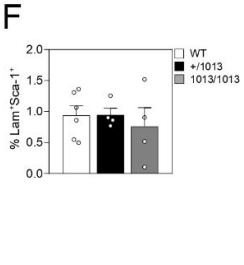
F
% Lam+Sca-1+
WT
+/1013
1013/1013

Fig. S3. Cxcr4^{1013} knockin mice display preserved proportion of BM arteriolar cells. (A) Relative contribution of CD45.2^{+} and CD45.1^{+} cells to B cells (CD19^{+}), myeloid cells (CD11b^{+}), and T cells (CD4^{+}) in the peripheral blood of CD45.1^{+}/CD45.2^{+} WT recipient mice 3 weeks after competitive BM transplantation. n=2 independent experiments for a total of 5 WT, 4 +/1013, and 4 1013/1013 donor mice. **(B)** Representative BM sections from WT mice stained for Flt3 and c-Kit by RNA-scope and for Sca-1 and Laminin by immunofluorescence. The color code for markers used is indicated and image obtained after merging signals corresponding to the different markers is shown. Nuclei are labelled with DAPI (blue). MPP4 defined as c-Kit^{+}Sca-1^{+}Flt3^{+} are highlighted in yellow on merged image. **(C)** Strategy to identify MPP4 on BM sections as in (B) by combining in situ hybridization assay RNA-scope and immunofluorescence staining. MPP4 defined as c-Kit^{+}Sca-1^{+}Flt3^{+} are highlighted in yellow. Scale bars, 10 μm. **(D)** Spatial distribution analysis of MPP4 cells using nearest neighbor index (NNI). n= 3 independent determinations for a total of 6 WT, 4 +/1013, and 4 1013/1013 mice. Mann–Whitney U test was used to determine absence of statistical significance (p=0.2571). **(E)** Representative BM section from WT mice showing arteriolar cells defined as Lam^{+}Sca-1^{+} and highlighted in purple. n= 3 independent experiments for a total of 6 WT, 4 +/1013, and 4 1013/1013 mice. Scale bar, 20 μm. **(F)** Proportions of arteriolar cells detected by immunofluorescence in the BM sections from WT and knockin mice. n= 3 independent experiments for a total of 6 WT, 4 +/1013, and 4 1013/1013 donor mice. $^{\#}$ $P < 0.05$; $^{\#\#\#}$ $P < 0.0005$ for Kruskal–Wallis tests; * $P < 0.05$; ** $P < 0.005$ for Dunn's test.

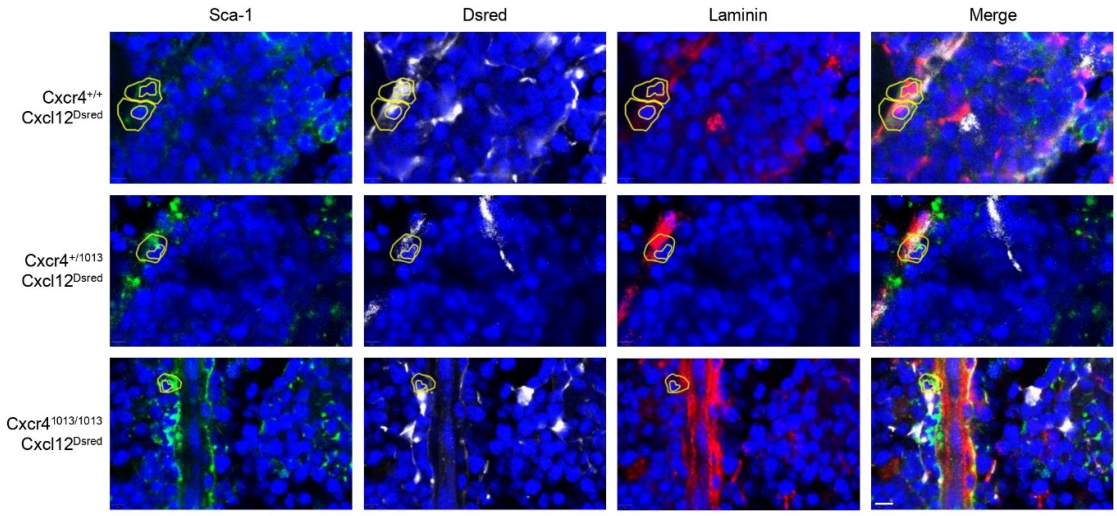

Fig. S4. Arteriolar cells express Cxcl12 independently of their *Cxcr4* mutational status. **(A)** Representative BM sections from *Cxcr4*$^{+/+}$*Cxcl12*^{Dsred}, *Cxcr4*$^{+/1013}$*Cxcl12*^{Dsred}, and *Cxcr4*$^{1013/1013}$*Cxcl12*^{Dsred} mice showing Sca-1 immunofluorescence, Dsred, Laminin immunofluorescence. Nuclei are labelled with DAPI (blue). MPP4 cells are outlined in yellow. BM sections are representative of n= 3 independent determinations for a total of 3 mice per group. Scale bar, 5 µm.

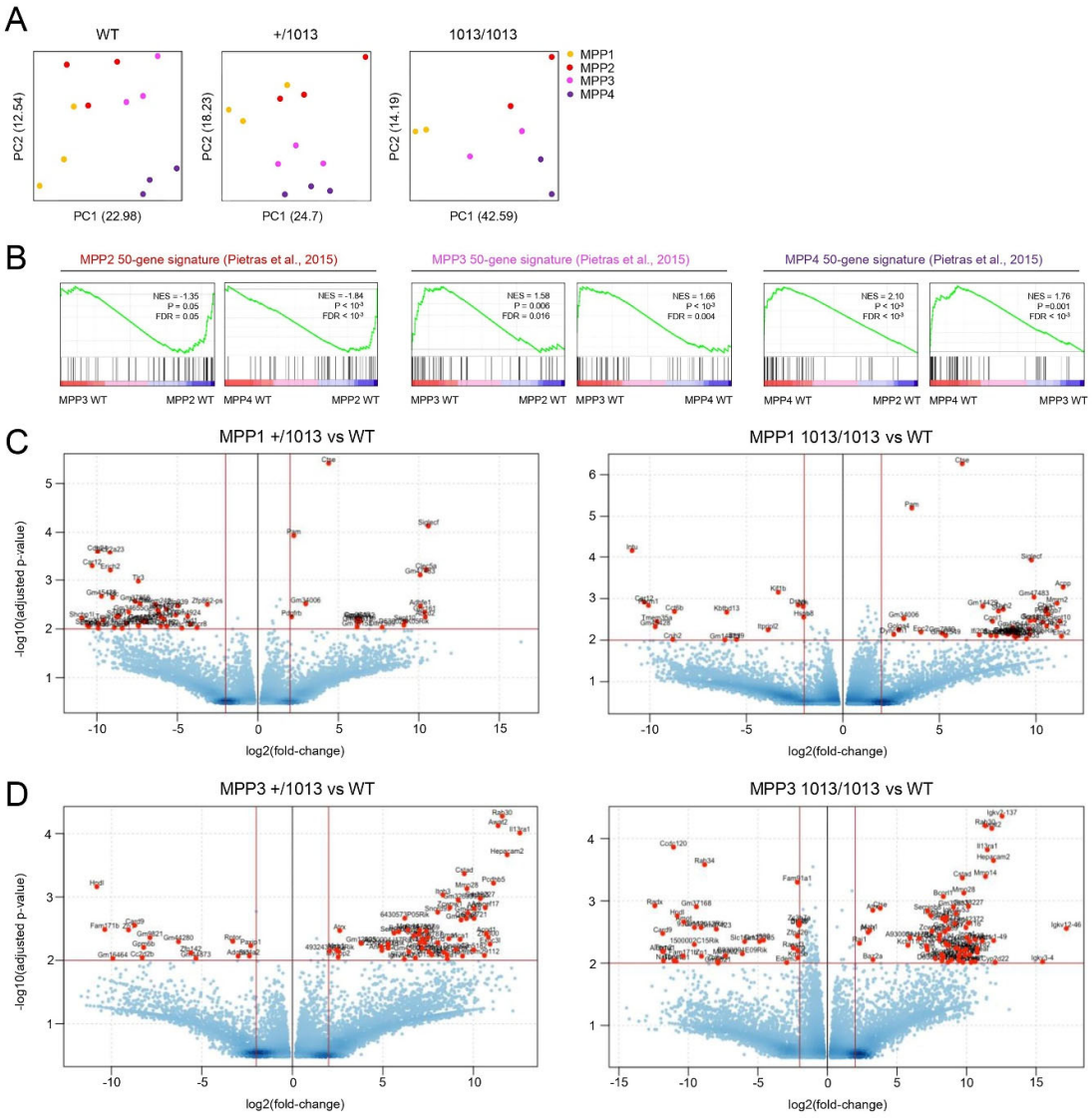

Fig. S5. MPP subsets do not share similar requirements for the Cxcl12-Cxcr4 signaling axis to maintain their molecular identity. (A) PCA of RNA-seq gene expression data obtained from the indicated MPP subpopulations in WT and knockin mice. **(B)** GSEA for MPP2-, MPP3- and MPP4-gene specific signatures between the indicated WT subpopulations. **(C)** Volcano plots of differentially expressed genes in +/1013 (left) vs. WT (right) MPP1 and in 1013/1013 (left) vs. WT (right) MPP1. Genes highly differentially expressed (log2FC(Cxcr4^{1013} knockin vs WT MPP1) > 2; -log10(adjusted p-value) > 2) are shown in red. **(D)** Volcano plot of differentially expressed genes in +/1013 vs. WT MPP3 and in 1013/1013 vs. WT MPP3. Genes highly differentially expressed (log2FC(Cxcr4^{1013} knockin vs WT MPP3) > 2; -log10(adjusted p-value) > 2) are shown in red.

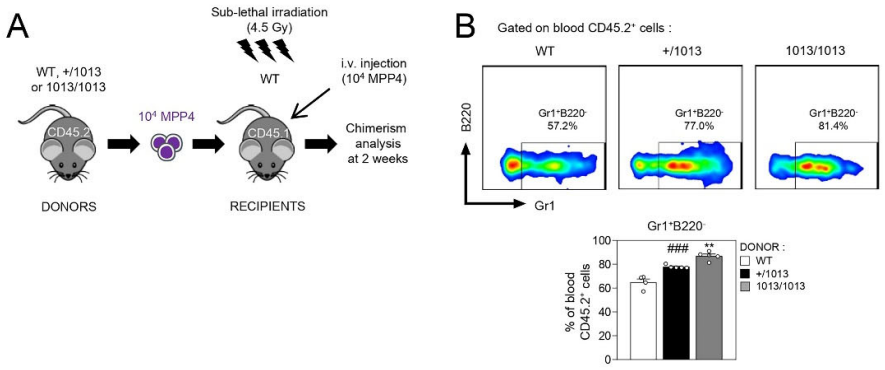

Fig. S6. Increased myeloid output in the peripheral blood of Cxcr4^{1013} knockin MPP4-chimeric mice. (A) In vivo differentiation assays workflow. **(B)** Proportions of donor CD45.2^{+} (WT, +/1013, or 1013/1013) myeloid cells (Gr1^{+}B220^{-}) recovered from the blood of CD45.1^{+} recipients two weeks after the transplantation. All displayed results are represented as means ± SEM and are from n= 2 independent experiments for a total of 4 WT, 5 +/1013, and 5 1013/1013 donor mice. $^{###}$ P < 0.0005 for Kruskal–Wallis tests; ** P < 0.005 for Dunn's test compared with WT.

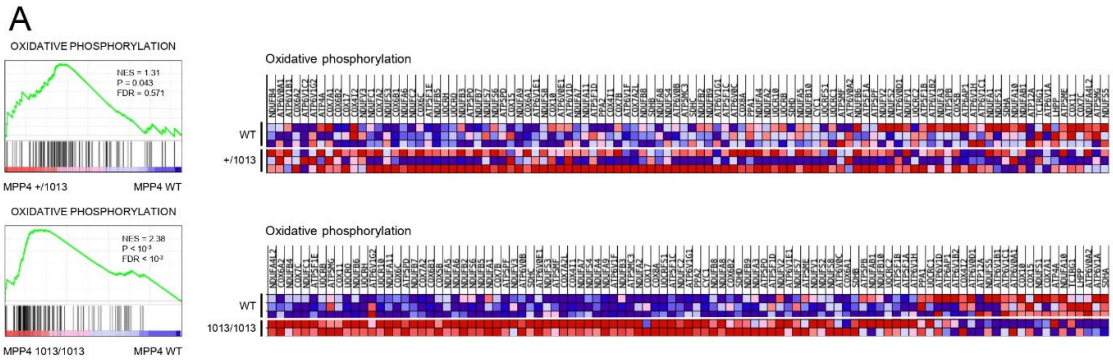
A
OXIDATIVE PHOSPHORYLATION
NES = 1.31
P = 0.043
FDR = 0.571
MPP4 +/1013
MPP4 WT
Oxidative phosphorylation
WT
+/1013
OXIDATIVE PHOSPHORYLATION
NES = 2.38
P < 10-3
FDR < 10-3
MPP4 1013/1013
MPP4 WT
Oxidative phosphorylation
WT
1013/1013

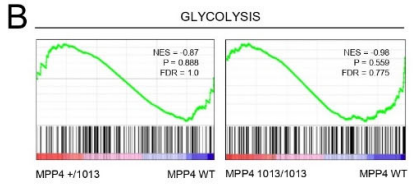
B
GLYCOLYSIS
NES = -0.87
P = 0.888
FDR = 1.0
NES = -0.98
P = 0.559
FDR = 0.775
MPP4 +/1013
MPP4 WT
MPP4 1013/1013
MPP4 WT

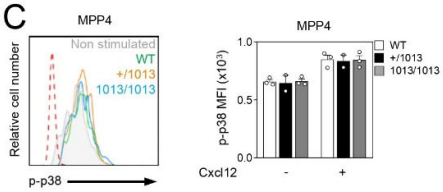
C
MPP4
Non stimulated
WT
+/1013
1013/1013
Relative cell number
p-p38
MPP4
p-p38 MFI (x10³)
WT
+/1013
1013/1013
Cxcl12

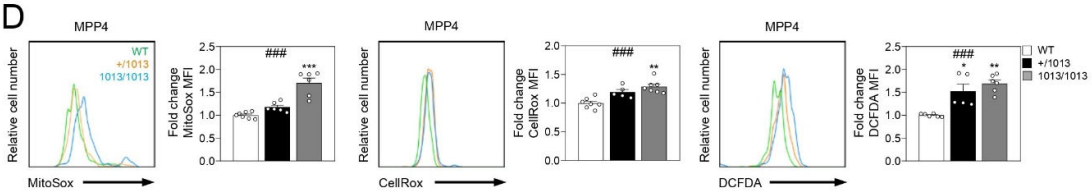
D
MPP4
WT
+/1013
1013/1013
Relative cell number
MitoSox
Fold change MitoSox MFI
###
***
MPP4
Relative cell number
CellRox
Fold change CellRox MFI
###
**
MPP4
Relative cell number
DCFDA
Fold change DCFDA MFI
###
**
WT
+/1013
1013/1013

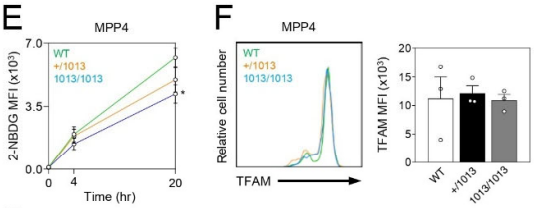
E
MPP4
WT
+/1013
1013/1013
2-NBDG MFI (x10³)
Time (hr)
F
MPP4
WT
+/1013
1013/1013
Relative cell number
TFAM
TFAM MFI (x10³)

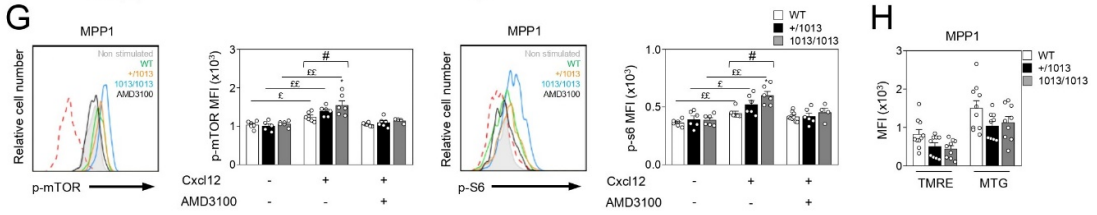
G
MPP1
Non stimulated
WT
+/1013
1013/1013
AMD3100
Relative cell number
p-mTOR
p-mTOR MFI (x10³)
Cxcl12
AMD3100
MPP1
Relative cell number
p-S6
p-S6 MFI (x10³)
WT
+/1013
1013/1013
H
MPP1
MFI (x10³)
TMRE
MTG

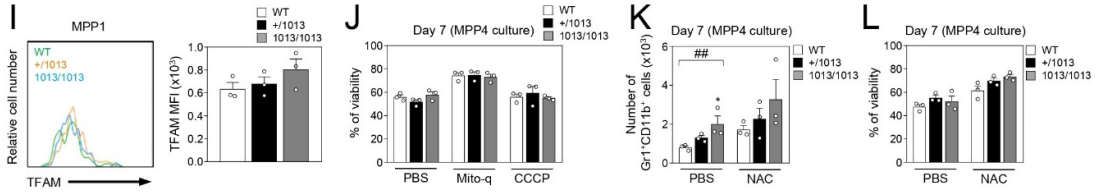
I
MPP1
WT
+/1013
1013/1013
Relative cell number
TFAM
TFAM MFI (x10³)
J
Day 7 (MPP4 culture)
% of viability
PBS
Mito-q
CCCP
K
Day 7 (MPP4 culture)
Number of Gr1+CD11b+ cells (x10³)
PBS
NAC
L
Day 7 (MPP4 culture)
% of viability
PBS
NAC

Fig. S7. Cxcr4^{1013} knockin MPP4 produce higher amounts of ROS and display reduce glucose uptake. (A) RNAseq-based GSEA for the OXPHOS signature in +/1013 vs. WT MPP4 and in 1013/1013 vs. WT MPP4. Heatmaps showing normalized dye intensity for the expression of genes involved in the OXPHOS signature in WT vs Cxcr4^{1013} knockin MPP4. **(B)** RNAseq-based GSEA for glycolysis signatures in WT and knockin MPP4. **(C)** Representative histograms for intracellular detection of phosphorylated p38 (p-p38) in sorted MPP4 from the marrow fraction of WT and knockin mice. Fluorescence in absence of phospho-p38 antibody (dashed line) or Cxcl12 stimulation (gray histogram) are shown. MFI values for p-p38 were determined by flow cytometry. n= 2 independent experiments for a total of 3 WT, 2 +/1013, and 3 1013/1013 mice. **(D)** Representative histograms for intracellular detection of ROS by flow cytometry in WT and knockin MPP4. Bar graphs denote the fold change in MitoSox, CellRoxDeepRed and DCFDA MFI values compared with those obtained in WT MPP4. n= 3 independent experiments for a total of 7 WT, 6 +/1013, and 6 1013/1013 mice (MitoSox), n= 3 independent experiments for a total of 7 WT, 5 +/1013, and 7 1013/1013 mice (CellRox), or n= 3 independent experiments for a total of 6 WT, 5 +/1013, and 6 1013/1013 mice (DCFDA). **(E)** MFI values for 2-NBDG determined by flow cytometry. n= 3 independent experiments for a total of 6 WT, 4 +/1013, and 6 1013/1013 mice. **(F)** Representative histograms for TFAM staining and MFI values in MPP4 from marrow fraction of WT and knockin mice. n= 3 independent experiments for a total of 3 mice per group. **(G)** Representative histograms for intracellular detection of phosphorylated mTOR (p-mTOR) and phosphorylated S6 (p-S6) in MPP1 from the marrow fraction of WT and knockin mice. Fluorescence in the absence of p-mTOR or p-S6 antibody (dashed line) or Cxcl12 stimulation (gray histogram) or in the presence of Cxcl12 and AMD3100 (black histogram) are shown. MFI values for p-mTOR and p-S6 were determined by flow cytometry. n= 3 independent experiments for a total of 6 mice per group (no AMD3100) or n= 3 independent experiments for a total of 6 WT, 6 +/1013, and 4 1013/1013 mice (with AMD3100). **(H)** MFI values for TMRE and MTG in WT and knockin MPP1. n= 3 independent experiments for a total of 10 WT, 9 +/1013, and 9 1013/1013 mice. **(I)** Representative histograms for TFAM staining and MFI values in MPP1 from marrow fraction of WT and knockin mice. n= 3 independent experiments for a total of 3 mice per group. **(J)** Viability in WT or knockin MPP4 cultures in the presence or absence of Mito-q and CCCP assessed at day 7 by flow cytometry using the Live/Dead dye. n= 3 independent experiments for a total of 3 mice per group. **(K and L)** Absolute numbers of mature myeloid cells ($Gr1^+CD11b^+$, K) and viability (L) were assessed at day 7 in WT or knockin MPP4 cultures in the presence or absence of NAC. n = 3 independent experiments with 3 mice per group. $^{\#}$ $P < 0.05$; $^{\#\#}$ $P < 0.005$; $^{\#\#\#}$ $P < 0.0005$ for Kruskal–Wallis tests; * $P < 0.05$; ** $P < 0.005$; *** $P < 0.0005$ for Dunn's test; $^{£}$ $P < 0.05$; $^{££}$ $P < 0.005$ for Mann-Whitney's test.

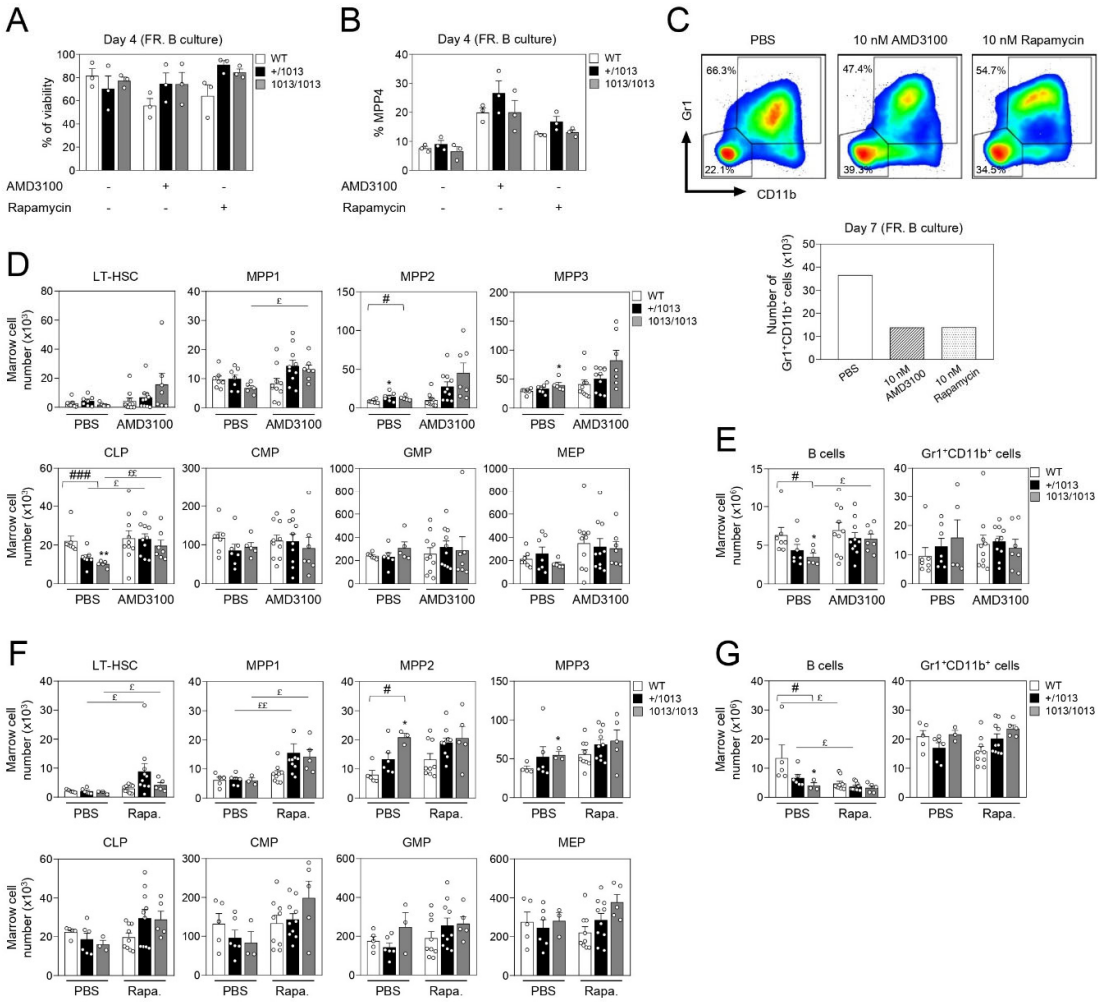
A
Day 4 (FR. B culture)
% of viability
WT
+/1013
1013/1013
AMD3100
Rapamycin
B
Day 4 (FR. B culture)
% MPP4
C
PBS
10 nM AMD3100
10 nM Rapamycin
66.3%
22.1%
47.4%
39.3%
54.7%
34.5%
Gr1
CD11b
Day 7 (FR. B culture)
Number of Gr1+CD11b+ cells (x10³)
D
LT-HSC
MPP1
MPP2
MPP3
CLP
CMP
GMP
MEP
Marrow cell number (x10³)
PBS
AMD3100
E
B cells
Gr1+CD11b+ cells
Marrow cell number (x10⁶)
F
Rapa.
G

Fig. S8. Chronic blockade of Cxcr4-dependent signaling in Cxcr4^{1013} knockin mice corrects the number of CLPs and mature B cells within BM. (A and B) Viability (A) and proportions of MPP4 (B) in WT or Cxcr4^{1013} knockin MPP4 cultures in the presence or absence of AMD3100 or rapamycin assessed at day 4 by flow cytometry. n= 3 independent experiments for a total of 3 mice per group. **(C)** Representative flow cytometric analyses comparing the frequencies of Gr1^{-}CD11b^{-} and Gr1^{+}CD11b^{+} cells at day 7 in TMRE^{low} (fraction B) MPP4 cultures in the presence or absence of AMD3100 or rapamycin. The graph shows absolute numbers of mature myeloid cells (Gr1^{+}CD11b^{+}) assessed at day 7. **(D)** Absolute numbers of LT-HSCs, MPP1-3, CLPs, CMPs, GMPs and MEPs were determined by flow cytometry in the marrow fraction of AMD3100-treated WT and knockin mice. n= 3 independent experiments for a total of 7 WT, 7 +/1013, and 5 1013/1013 mice (PBS condition) and a total of 10 WT, 10 +/1013, and 7 1013/1013 mice (AMD3100 condition). **(E)** Absolute numbers of B cells (CD19^{+}B220^{+}) and mature myeloid cells (Gr1^{+}CD11b^{+}) in the marrow fraction of treated mice. n= 3 independent experiments for a total of 7 WT, 7 +/1013, and 5 1013/1013 mice (PBS condition) and a total of 10 WT, 10 +/1013, and 7 1013/1013 mice (AMD3100 condition). **(F)** Absolute numbers of LT-HSCs, MPP1-3, CLPs, CMP, GMPs, and MEPs determined by flow cytometry in the marrow fraction of treated WT and knockin mice 2h after the last injection of rapamycin. n= 3 independent experiments for a total of 5 WT, 6 +/1013, and 3 1013/1013 mice (PBS condition) and a total of 9 WT, 10 +/1013 and 5 1013/1013 mice (Rapamycin condition). **(G)** Absolute numbers of B cells and mature myeloid cells in the marrow fraction of treated mice. n= 3 independent experiments for a total of 5 WT, 6 +/1013, and 3 1013/1013 mice (PBS condition) and a total of 9 WT, 10 +/1013, and 5 1013/1013 mice (rapamycin condition). $^{\#}$ $P < 0.05$; $^{\#\#\#}$ $P < 0.0005$ for Kruskal–Wallis tests; * $P < 0.05$; ** $P < 0.005$; for Dunn's test; $^{£}$ $P < 0.05$; $^{££}$ $P < 0.005$ for Mann-Whitney's test.

Table S1. Biomark principal component analysis contributing genes related to Fig 5.

Genes	PC1	PC2
Mpo	22.9410772293186	0.0226051554014014
Irf8	26.7415577574601	3.12993943231947
Cebpa	4.8618201396235	39.8904666219647
Gfi1b	0.305843078631275	42.870602086591
Ikzf1	11.6849571840968	5.4133811606772
Il7r	2.79762481876075	0.552813189945707
Dntt	19.9260608421189	8.06212105674224
Bach2	10.7410589499902	0.0580712963582981

Table S2. List of primers used for the BioMark assay related to Fig. 5 and fig. S1.

Genes	Primers
MPP markers	
Cd48	Mm00455932_m1
Slamf1	Mm00443316_m1
Flt3	Mm00439016_m1
Irf8	Mm00492567_m1
Lymphomyeloid differentiation	
Ikzf1	Mm01187880_m1
Il7r	Mm00434295_m1
Dntt	Mm00493500_m1
Bach2	Mm00464379_m1
Mpo	Mm00447886_m1
Cebpa	Mm00514283_s1
Gfi1b	Mm00492318_m1
Irrelevant genes (negative controls)	
Pax5	Mm00435501_m1
Cd3e	Mm00599684_g1
Housekeeping gene	
Actb	Mm01205647_g1

Table S3. List of antibodies used for immunofluorescence related to Fig. 6.

Antibody	Origin	Conjugate	Supplier
Tomm20	Rabbit	Uncoupled	Thermo Fischer Scientific
IgG (Secondary Antibody)	Goat	Alexa Fluor 555	Thermo Fischer Scientific

Data file S1. Complete list of increased and decreased ATAC-seq peaks in 1013/1013 MPP1 related to Fig. 2.

Data file S2. Complete GO analysis of genes associated with decreased ATAC-seq peaks in Cxcr4^{1013} knockin MPP1 related to Fig. 2.

Data file S3. Complete GO analysis of genes associated with increased ATAC-seq peaks in Cxcr4^{1013} knockin MPP1 related to Fig. 2.

Data file S4. List of HOMER known motifs decreased in Cxcr4^{1013} knockin MPP1 related to Fig. 2.

Data file S5. List of HOMER known motifs increased in Cxcr4^{1013} knockin MPP1 related to Fig. 2.

Data file S6. Complete GO analysis of genes associated with decreased ATAC-seq peaks in Cxcr4^{1013} knockin MPP4 related to Fig. 2.

Data file S7. Complete list of decreased and increased ATAC-seq peaks in 1013/1013 MPP4 related to Fig. 2.

Data file S8. Complete GO analysis of genes associated with increased ATAC-seq peaks in Cxcr4^{1013} knockin MPP4 related to Fig. 2.

Data file S9. List of HOMER known motifs decreased in Cxcr4^{1013} knockin MPP4 related to Fig. 2.

Data file S10. List of HOMER known motifs increased in Cxcr4^{1013} knockin MPP4 related to Fig. 2.

Data file S11. List of genes significantly increased or decreased in Cxcr4^{1013} knockin MPP4 related to Fig. 4.

Data file S12. Complete GO analysis of genes that increased or decreased in Cxcr4^{1013} knockin MPP4 related to Fig. 4.